Acta Crystallographica Section B
**Structural Science**
ISSN 0108-7681

# The low-temperature phase III structure and phase transition behaviour of cyclohexanone

**Richard M. Ibberson**

ISIS Facility, CCLRC – Rutherford Appleton Laboratory, Chilton, Didcot, Oxfordshire OX11 0QX, England

Correspondence e-mail: r.m.ibberson@rl.ac.uk

Received 8 September 2005
Accepted 27 April 2006

The crystal structure of phase III of perdeuterocyclohexanone, $C_6D_{10}O$, has been determined at 5 K using high-resolution neutron powder diffraction. Below its melting point of 245 K cyclohexanone forms a plastic crystal in the space group $Fm\bar{3}m$. On cooling below 225 K the crystal transforms to the monoclinic phase III structure in the space group $P2_1/n$. The orthorhombic phase II structure exists under high pressure, but the triple point for all three phases is close to atmospheric pressure. Details of the phase II structure are also reported at 4.8 kbar (273 K) and ambient pressure. The phase behaviour of the compound and isotope effects are discussed.

## 1. Introduction

Cyclohexanone is a relatively simple organic molecular compound, but it exhibits notable structural polymorphism over a narrow range of temperature and pressure (Fig. 1). It is one of a number of medium-ring cyclic ketones that exhibit order–disorder transitions (Fried, 1973) and its phase behaviour has been studied using a number of experimental techniques. These include calorimetry (Nakamura *et al.*, 1980; Würflinger, 1980; Würflinger & Kreutzenbeck, 1978), dielectric constant measurements (Würflinger, 1980; Crowe & Smyth, 1951), NMR studies (Huang *et al.*, 1993; Fried, 1973), and Raman and IR spectroscopy (Huang *et al.*, 1993).

At ambient pressure, cyclohexanone melts at 245 K and undergoes a phase transition at 225 K. The low entropy of fusion (5.41 J $K^{-1}$ $mol^{-1}$) determined by Nakamura *et al.* (1980) compared with the entropy of transition (39.22 J $K^{-1}$ $mol^{-1}$) is indicative of an order–disorder transition. The NMR results of Huang *et al.* (1993) also support this conclusion with the observation of rapid isotropic reorientation of the molecules in phase I and discrete external modes in the low-frequency Raman spectrum at 73 K, implying an ordered phase III structure. Phase II exists under high pressure (Würflinger & Kreutzenbeck, 1978), however, the triple point for all three phases coincides with atmospheric pressure within the limits of experimental error. Indeed differential thermal analysis of cyclohexanone on cooling and heating (Nakamura *et al.*, 1980) shows a very different behaviour. In addition to a large hysteresis effect, a much broader transition was observed on heating, which was attributed to a two-stage transition process which most likely corresponds to an observation of phase II at ambient pressure.

Despite this interest in the crystalline forms of cyclohexanone and the need to understand simple systems in order to derive the generic factors controlling the phase behaviour in other more complex molecular compounds, little structural

information is known on these low-temperature phases. An early X-ray powder study (Hassel & Sommerfeldt, 1938) reported a face-centred cubic cell for phase I with a lattice constant of 8.61 Å at 218 K. Phases II and III have remained elusive not least due to the tendency for single crystals to shatter due to the volume change on passing through the phase transition at 225 K and the apparent need for (modest) high pressures to stabilize phase II. The advent of techniques for the *in situ* growth of single crystals from liquids (see, for example, Boese & Nussbaumer, 1994; Boese *et al.*, 2003; Pardoe *et al.*, 2003) can provide a route for structural studies that bypass the potentially destructive first-order transition. Shallard-Brown *et al.* (2005) successfully grew a single crystal of cyclohexanone at 180 K by careful zone melting and reported an ordered orthorhombic structure in the space group $P2_12_12_1$ at 150 K. Analysis of the low-frequency Raman spectrum (Huang *et al.*, 1993) suggests an orthorhombic non-centrosymmetric structure for phase III at 73 K, which is apparently in agreement with the single-crystal observations. The spectroscopic observations, however, may have been potentially misleading as the previously reported orthorhombic structure is shown here to correspond to phase II.

The motivation for the present study is therefore to carry out a more detailed study of the known phases in the region of the order–disorder transition and to elucidate the remaining unknown structure at elevated pressure. High-resolution neutron powder diffraction provides a useful and complementary alternative to single-crystal X-ray diffraction in these situations. High-quality powder samples are trivial to prepare for compounds with melting points down to *ca* 150 K (Ibberson, 1996) and using powder samples the problems associated with first-order phase transitions are largely avoided. Here we report the crystal structure of perdeuterocyclohexanone at a series of temperatures between 5 and the 225 K transition and report, to the best of our knowledge, the first full determination of the structure of phase III.

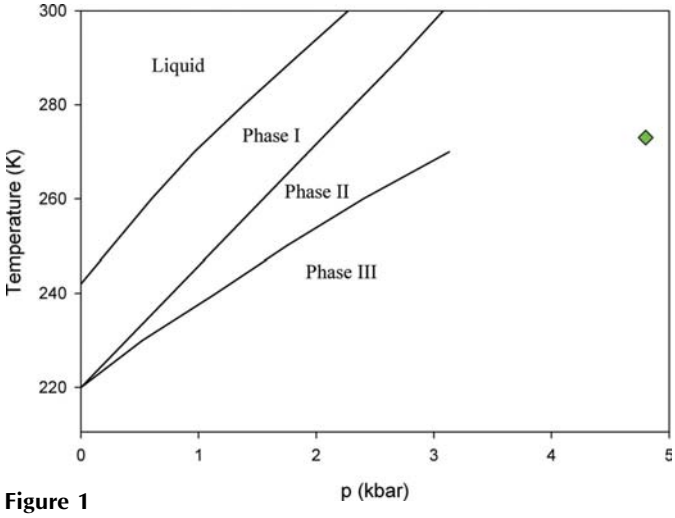


**Figure 1**
The *p–T* phase diagram of cyclohexanone (after Würflinger & Kreutzenbeck, 1978). The diamond denotes the location of the high-pressure phase II structure of perdeuterocyclohexanone described in the current study.

## 2. Experimental

Cyclohexanone is a clear colourless liquid with a melting point of 245 K and a boiling point of 429 K. To avoid the problems due to the high incoherent neutron scattering cross section of hydrogen, a sample of perdeuterocyclohexanone (98+% atom D), (I), was obtained from C/D/N Isotopes Inc. for the neutron diffraction study.

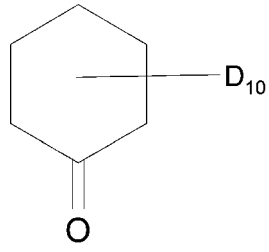


(I)

### 2.1. Neutron powder diffraction measurements

A 5 g sample of $C_6D_{10}O$ was frozen in a stainless steel mortar cooled using liquid nitrogen and then ground by hand to a fine powder before transferring to an 11 mm diameter vanadium sample can held at liquid-nitrogen temperature. The sample was loaded in a vanadium-tailed 'orange' cryostat and annealed at 210 K before slowly cooling to 5 K. Time-of-flight neutron powder diffraction data were recorded using the high-resolution powder diffractometer (HRPD; Ibberson *et al.*, 1992) at ISIS for 200 μAh (*ca* 11 h) at backscattering, $\langle 2\theta \rangle = 168^\circ$, over a time-of-flight range of between 20 and 220 ms, corresponding to a *d*-spacing range of between 0.4 and 4.4 Å. Under these experimental settings the instrumental resolution, $\Delta d/d$, is approximately constant and equal to $8 \times 10^{-4}$. Lower resolution data were recorded simultaneously in the 90 and 30° detector arrays out to *d* spacings of some 16 Å for cell indexing purposes. Variable-temperature data sets were then recorded over a time-of-flight range of between 30 and 130 ms, corresponding to a *d*-spacing range of between 0.6 and 2.6 Å at backscattering. The data collection period for these runs was on average 15 μAh (*ca* 25 min).

Data at high pressure were recorded subsequently from the same sample loaded, in liquid form, in a 'null-scattering' TiZr alloy gas-pressure cell. The pressure cell utilizes a Bridgeman seal and has a sample volume of approximately 1 $cm^3$. Glass wool was inserted into the cell in an attempt to promote the formation of fine crystallites and minimize potential problems of texture on freezing the liquid. Hydrostatic pressure is achieved by means of an He gas intensifier system fed to the cell *via* capillary tubing. The gas cell apparatus is designed for use in a standard cryostat and can be controlled to ±25 bar up to a maximum operating pressure of 4.8 kbar. A single measurement was made at the maximum operating pressure at a temperature of 273 K. Data were recorded using the 90° detector bank over the time-of-flight range 20–220 ms corre-

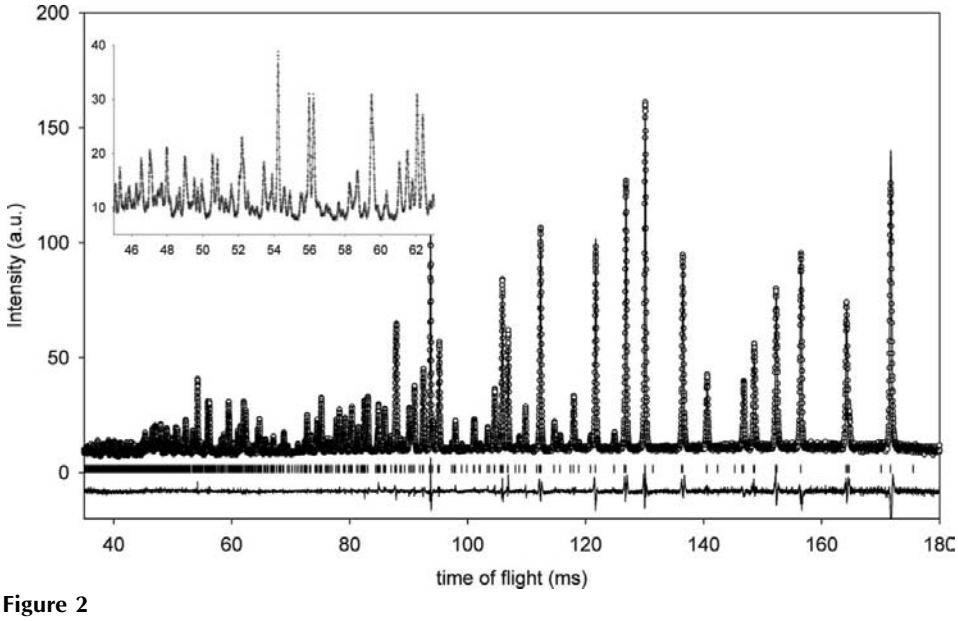


**Figure 2**
The final Rietveld refinement plot of phase III at 5 K, showing observed (o), calculated (line) and difference (lower) profiles. Vertical bar markers indicate calculated Bragg peak positions. The equivalent *d*-spacing range corresponds to 0.7–3.6 and 0.9–1.4 Å for the inset.

**Table 1**
Crystallographic and refinement details for cyclohexanone phase III.

| | |
|---|---|
| Crystal data | |
| Chemical formula | $C_6D_{10}O$ |
| $M_r$ | 108.14 |
| Cell setting, space group | Monoclinic, $P2_1/n$ |
| Temperature (K) | 5.0 |
| $a, b, c$ (Å) | 11.7105 (1), 7.1198 (1), 6.8621 (1) |
| $\beta$ (°) | 95.5627 (3) |
| $V$ (Å$^3$) | 569.45 (1) |
| $Z$ | 4 |
| $D_x$ (Mg m$^{-3}$) | 1.261 (1) |
| Radiation type | Time-of-flight neutron |
| Specimen form, colour | Cylinder (particle morphology: irregular powder), white |
| Specimen size (mm) | 25 × 11 |
| Data collection | |
| Diffractometer | HRPD |
| Data collection method | Specimen mounting: standard 11 mm diameter vanadium sample holder; time-of-flight range 20–220 ms |
| Total flight path (m), $\langle 2\theta \rangle$ (°) | 95.98, 168.329 |
| Refinement | |
| Refinement on | $F^2$ |
| $R$ factors and goodness of fit | $R_p$ = 0.047, $R_{wp}$ = 0.044, $R_{exp}$ = 0.024, $S$ = 1.86 |
| Wavelength of incident radiation (Å) | 0.83–9.01 |
| Excluded region(s) | None |
| Profile function | TOPAS TOF Profile function |
| No. of parameters | 99 |
| D-atom treatment | Fully refined (isotropic) |
| Weighting scheme | Based on measured s.u.'s |
| $(\Delta/\sigma)_{max}$ | 0.01 |

Computer programs used: ISIS Instrument control program (*ICP*), *TOPAS-Academic* (Coelho, 2000), Standard HRPD normalization routines, *ORTEP*3 (Farrugia, 1997), *PLATON* (Spek, 2003).

sponding, in this case, to a *d*-spacing range of between 0.6 and 6.4 Å at a resolution approximately constant and equal to 2 × $10^{-3}$.

A standard data reduction procedure was followed: the data were normalized to the incident-beam monitor profile and corrected for detector efficiency effects using a previously recorded vanadium spectrum. The high-pressure data set was further corrected for attenuation effects due to the pressure cell.

The diffraction patterns recorded at 5 K were indexed based on the positions of the first 25 peaks (2.5 < $d$ < 6.2 Å) using *DICVOL*91 (Boultif & Louër, 1991). A monoclinic cell was determined: $a$ = 11.710 (2), $b$ = 7.124 (2), $c$ = 6.864 (2) Å, $\beta$ = 95.55 (2)° and $V$ = 569.94 Å$^3$. All Bragg peaks could be indexed on the basis of this cell, indicating the sample was single phase. All data sets recorded on warming were satisfactorily refined on the basis of this monoclinic unit cell up to 225 K, at which point co-existence of the cubic [$a$ = 8.59879 (3) Å] phase I structure was observed. A number of experiments were subsequently performed quenching a cubic phase sample from 225 to 150 K at cooling rates of some 10–20 K min$^{-1}$. These invariably reproduced the monoclinic phase, however, additional peaks from a minor second phase were observed. This second phase could be indexed using an orthorhombic cell [150 K: $a$ = 5.3677 (4), $b$ = 7.0295 (4), $c$ = 15.147 (1) Å, $V$ = 571.54 Å$^3$] in agreement with the structure of Shallard-Brown *et al.* (2005) who report a cell volume of 574.63 Å$^3$ at the same temperature. A subsequent two-phase refinement of these data showed the weight fraction of the orthorhombic phase to be only 0.053 (1) in the sample.

The diffraction pattern recorded at high-pressure was indexed using *DICVOL*91, as described previously. In this case an orthorhombic cell was determined: $a$ = 5.306 (2), $b$ = 6.926 (2), $c$ = 15.084 (6) Å, $V$ = 554.36 Å$^3$. It was concluded, therefore, that phase II of cyclohexanone has an orthorhombic structure that transforms to a monoclinic structure in phase III.

The phase III structure was solved in the space group $P2_1/n$ by simulated annealing implemented by *TOPAS-Academic* (Coelho, 2000) using a rigid-body molecular template derived from the guest structure of cyclohexanone in a deoxycholic acid host (Popvitz-Biro *et al.*, 1985). The structure was then refined by the Rietveld method implemented by *TOPAS-Academic* without the use of constraints. Details of the refinement are given in Table 1[1] and the final profile fit is shown in Fig. 2. The variable-temperature data sets were

[1] Supplementary data for this paper are available from the IUCr electronic archives (Reference: WS5037). Services for accessing these data are described at the back of the journal.

**Table 3**
Refined unit-cell parameters for cyclohexanone as a function of temperature.

| Temperature (K) | $a$ (Å) | $b$ (Å) | $c$ (Å) | $\beta$ (°) | $V$ (Å$^3$) |
|---|---|---|---|---|---|
| Phase III | | | | | |
| 5 | 11.7095 (1) | 7.1186 (1) | 6.8616 (1) | 95.5636 (4) | 569.255 (4) |
| 25 | 11.7120 (1) | 7.1209 (1) | 6.8628 (1) | 95.5699 (6) | 569.653 (5) |
| 50 | 11.7199 (1) | 7.1337 (1) | 6.8670 (1) | 95.5695 (13) | 571.422 (10) |
| 75 | 11.7285 (1) | 7.1533 (1) | 6.8722 (1) | 95.5562 (12) | 573.849 (10) |
| 100 | 11.7376 (1) | 7.1790 (1) | 6.8780 (1) | 95.5334 (10) | 576.867 (9) |
| 150 | 11.7575 (1) | 7.2466 (1) | 6.8930 (1) | 95.4693 (11) | 584.627 (11) |
| 175 | 11.7658 (1) | 7.2806 (1) | 6.9004 (1) | 95.4362 (11) | 588.447 (11) |
| 195 | 11.7727 (1) | 7.3110 (1) | 6.9067 (1) | 95.4002 (10) | 591.817 (10) |
| 210 | 11.7766 (1) | 7.3315 (1) | 6.9110 (1) | 95.3759 (10) | 594.068 (10) |
| 215 | 11.7792 (1) | 7.3453 (1) | 6.9138 (1) | 95.3568 (12) | 595.575 (12) |
| 225 | 11.7822 (1) | 7.3635 (1) | 6.9173 (1) | 95.3310 (6) | 597.536 (4) |
| Phase II | | | | | |
| 130 | 5.3461 (4) | 7.0298 (6) | 15.1047 (14) | – | 567.67 (5) |
| 150 | 5.3678 (4) | 7.0295 (4) | – | – | 571.54 (5) |
| Phase I | | | | | |
| 225 | 8.59879 (3) | – | – | – | 635.787 (7) |

refined using a model based on the 5 K structure. In these refinements the atomic coordinates were fixed and the only structural parameters refined were the lattice constants and (three) isotropic temperature factors for C, D and O atoms, respectively.

## 3. Results and discussion

### 3.1. Phase III crystal structure

The asymmetric unit (Fig. 3) of the structure of phase III cyclohexanone comprises one complete molecule located on a general position and thus 17 independent atoms. The structure is characterized by molecules, stacked perpendicular to the plane of the six-membered ring, to form columns running parallel to the crystallographic $b$ axis (Fig. 4). Neighbouring molecules in these columns are linked by four short O···D contacts in the range 2.48–2.59 Å (Table 2). The structure also exhibits a CO···CO contact distance of 3.43 Å in an anti-parallel motif and is referred to as Type II by Allen *et al.* (1998). Shallard-Brown *et al.* (2005) report no strong intermolecular interactions in the phase II structure, however, there is a 2.61 Å contact in the structure between H62 and O7 which runs along the $2_1$ axis along the crystallographic $a$ axis. Type I CO···CO contacts (Allen *et al.*, 1998) of 3.35 Å, characterized by a perpendicular motif, are also evident in the structure and this shorter contact distance may well reflect the lack of competing CH···O contacts in the phase II structure.

The variation of the unit-cell parameters with temperature is given in Table 3 and the unit-cell volume is shown in Fig. 5. All parameters show a smooth variation until just before the 225 K transition and the cell-volume data are well fitted using a Debye model (Sayetat *et al.*, 1998) with the refined parameters $V_{0\,K}$ = 569.337 (1) Å and $\theta_D$ = 187.1 (2) K. Fig. 5 also shows the cell-volume data determined for phases I and II during the present study. There is a large (6.4%) increase in molecular volume from 149.38 to 158.95 Å$^3$ consistent with the first-order transition from phase III to the plastic phase I. The smaller molecular volume observed for phase II compared with phase III at 150 K, 142.89 and 146.16 Å$^3$, respectively, is similarly consistent with the indication that phase II is the more stable phase under pressure.

**Table 2**
Contact distances (Å) for cyclohexanone phase III.

| | | | |
|---|---|---|---|
| D22···O7$^{i}$ | 2.515 (3) | D52···O7$^{ii}$ | 2.481 (3) |
| D31···O7$^{iii}$ | 2.575 (3) | D62···O7$^{iv}$ | 2.591 (3) |

Symmetry codes: (i) $\frac{1}{2}-x,-\frac{1}{2}+y,\frac{3}{2}-z$; (ii) $x,y,1+z$; (iii) $\frac{1}{2}-x,\frac{1}{2}+y,\frac{3}{2}-z$; (iv) $\frac{1}{2}-x,-\frac{1}{2}+y,\frac{3}{2}-z$.

Within the crystal structure the cyclohexanone molecules exhibit a chair conformation ($C_1$ symmetry) with puckering parameters $Q$ = 0.545 (2) Å, $\theta$ = 9.0 (2)° and $\varphi$ = 185.4 (15)° (Cremer & Pople, 1975). These values are in agreement with

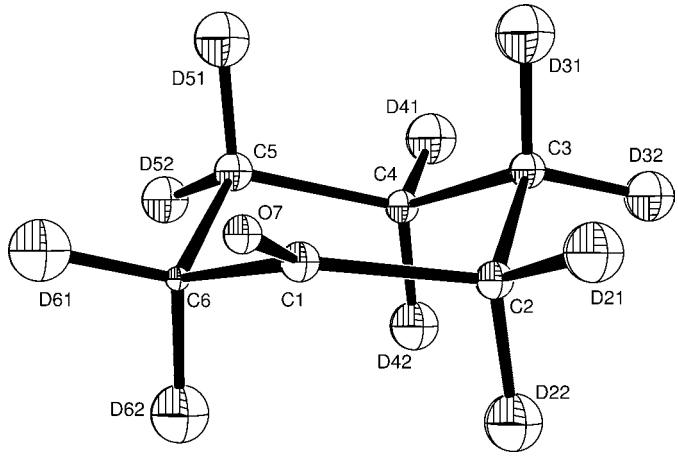


**Figure 3**
The asymmetric unit of cyclohexanone at 5 K, with isotropic displacement ellipsoids drawn at the 50% probability level.

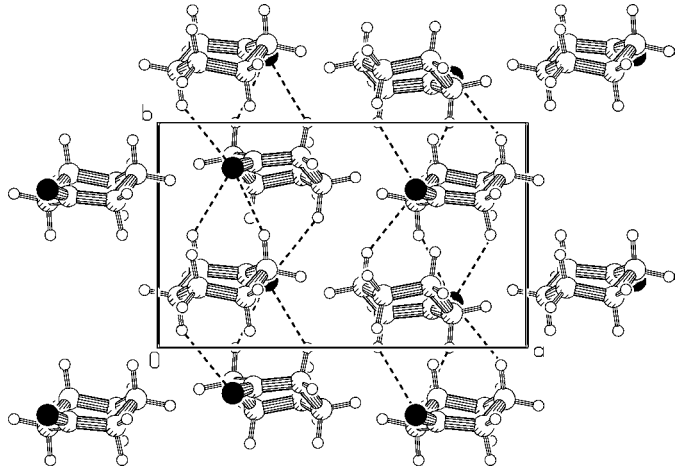


**Figure 4**
The crystal structure of phase III cyclohexanone, viewed down the crystallographic $c$ axis. Dotted lines denote O···D contacts listed in Table 2.

the predominant conformation observed in substituted cyclohexanone structures (Bocelli, 1981; Spek *et al.*, 1990). In fact, along with the structure of 2,6-dichlorocyclohexanone, Bocelli provides an analysis of 22 substituted cyclohexanone structures, of which 18 show a chair conformation of the cyclohexanone ring. Conformational studies on the isolated molecule by molecular mechanics (Langley *et al.*, 2001), *ab initio* density functional theory (DFT; Devlin & Stephens, 1999) and electron diffraction (ED; Dillen & Geize, 1980) report the chair form ($C_s$ symmetry) of cyclohexanone to be most stable. A comparison between experimental and calculated structures is shown in Table 4. The loss of the plane of symmetry in the molecule in the crystalline form is only marginally significant within experimental error, and bond and torsion angles are generally in good agreement. A restrained refinement in which chemically equivalent C—C bonds were kept equal to within 0.001 Å yields C1—C2, C2—C3 and C3—C4 bond lengths of 1.494, 1.523 and 1.530 Å, respectively. There is, however, a significant discrepancy when considering the $sp^2$-hybridized part of the ring. The discrepancy of some 0.02 Å in the C=O bond length between experiment [1.229 (3) Å determined from electron diffraction] and theory (1.209 Å) is also observed in the current study. For cyclohexanone phase III (5 K) the C=O bond length is 1.225 (3) Å and for phase II at 150 K the value is reported to be 1.213 (2) Å (Shallard-Brown *et al.*, 2005). Libration effects do play a role in the 150 K single-crystal study and a libration-corrected value for this bond length, calculated using *PLATON* (Spek, 2003), is 1.221 (3) Å. The experimentally determined values all agree within 0.008 Å (less than three standard deviations). Whilst the discrepancies between experiment and theory are only marginally significant within experimental error, this may indicate current limitations in the calculation of this key aspect of carbonyl compounds or simply be a result of crystal packing effects discussed above.

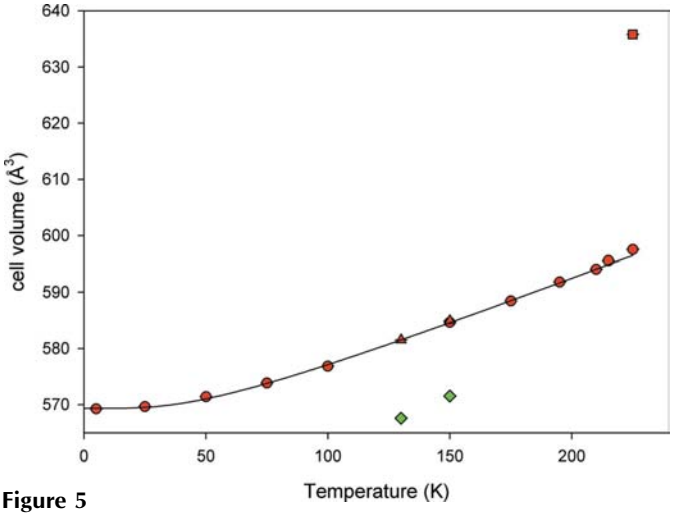


**Figure 5**
Variation of the unit-cell volume for cyclohexanone. Phase I is denoted by squares and phase II by diamonds. Data for phase III from the main experiment are denoted by circles and fitted to a Debye model (see text), and by triangles for the two-phase samples containing phase II.

**Table 4**
Experimental and calculated intramolecular bond lengths (Å) and angles (°) for cyclohexanone.

| | Phase III (5 K) | Phase II (150 K)† | DFT‡ | ED§ |
|---|---|---|---|---|
| O7—C1 | 1.225 (3) | 1.221 (3) | 1.209 | 1.229 (3) |
| C1—C2 | 1.494 (3) | 1.511 (2) | 1.514 | 1.503 (4) |
| C1—C6 | 1.495 (3) | 1.523 (2) | – | – |
| C2—C3 | 1.526 (3) | 1.541 (3) | 1.534 | 1.542 (2) |
| C3—C4 | 1.543 (3) | 1.529 (3) | 1.525 | 1.545 |
| C4—C5 | 1.517 (3) | 1.533 (3) | – | – |
| C5—C6 | 1.529 (3) | 1.542 (3) | – | – |
| $\langle$C—C$\rangle_{av}$ | 1.517 (20)¶ | 1.530 (12)† | – | – |
| $\langle$C—H$\rangle_{av}$ | 1.102 (12)¶ | 0.98 | 1.109 | 1.088 (5) |
| O7—C1—C2 | 122.5 (2) | 122.61 (15) | 122.4 | – |
| O7—C1—C6 | 122.0 (2) | 121.93 (15) | – | – |
| C2—C1—C6 | 115.51 (17) | 115.45 (14) | 115.2 | 115.3 (3) |
| C1—C2—C3 | 111.84 (17) | 112.29 (15) | 111.9 | 111.5 (1) |
| C2—C3—C4 | 110.62 (16) | 111.63 (15) | 111.6 | 110.8 (2) |
| C3—C4—C5 | 110.07 (17) | 110.85 (16) | 111.1 | 110.8 (2) |
| C4—C5—C6 | 110.21 (17) | 111.04 (15) | – | – |
| C1—C6—C5 | 111.97 (17) | 111.65 (13) | – | – |
| O7—C1—C6—C5 | 131.6 (2) | 132.53 (17) | – | – |
| O7—C1—C2—C3 | −132.3 (2) | −133.44 (17) | 131.4 | 128.3 |
| C6—C1—C2—C3 | 49.0 (2) | 47.68 (19) | 48.7 | 51.7 |
| C2—C1—C6—C5 | −49.8 (2) | −48.58 (19) | – | – |
| C2—C3—C4—C5 | 58.5 (2) | 56.8 (2) | 563 | 53.0 |
| C3—C4—C5—C6 | −58.9 (2) | −57.8 (2) | – | – |
| C4—C5—C6—C1 | 54.0 (2) | 52.8 (2) | – | – |
| C1—C2—C3—C4 | −52.4 (2) | −51.1 (2) | 51.8 | 56.3 |

† After Shallard-Brown *et al.* (2005). Bond-length corrections for libration effects have been applied. ‡ After Devlin & Stephens (1999). B3PW91 using the TZ2P basis set. § After Dillen & Geize (1980). In this study the C3—C4 bond is constrained relative to C2—C3 and the torsion angles were not refined as independent variables. ¶ The r.m.s. and not the mean standard deviations are shown in parentheses.

### 3.2. Phase II crystal structure at high pressure

A representative diffraction pattern of the phase II structure at high pressure is shown in Fig. 6, including a calculated pattern based on the single-crystal structure. The pattern is dominated by three strong peaks, which are indicative of a highly textured sample which could not be improved following various thermal cycling routes. Analysis of the pattern showed that the dominant peaks correspond to (0*kl*) reflections. The phase II structure is composed of molecules lying essentially parallel to the crystallographic *bc* plane and so the observation of preferred orientation under pressure coincident with this direction in the structure is not surprising. Pattern fitting using the Pawley method (Pawley, 1981) showed the sample to be a single phase with cell constants: $a$ = 5.3141 (3), $b$ = 6.9387 (2), $c$ = 15.1023 (5) Å, $V$ = 556.87 (4) Å$^3$. A full structural refinement, including attempts to model the texture, were largely unsuccessful. Although confirming the $P2_12_12_1$ structure is the stable form at 4.8 kbar and 273 K, no reliable atomic structural parameters can be reported.

### 3.3. Phase transition behaviour

The present structural studies and those from the recent single-crystal study of Shallard-Brown *et al.* (2005) confirm the previous suggestions (Nakamura *et al.*, 1980) that phase II of cyclohexanone has a limited stability field at ambient pressure. It seems unlikely, therefore, that the Raman studies of Huang

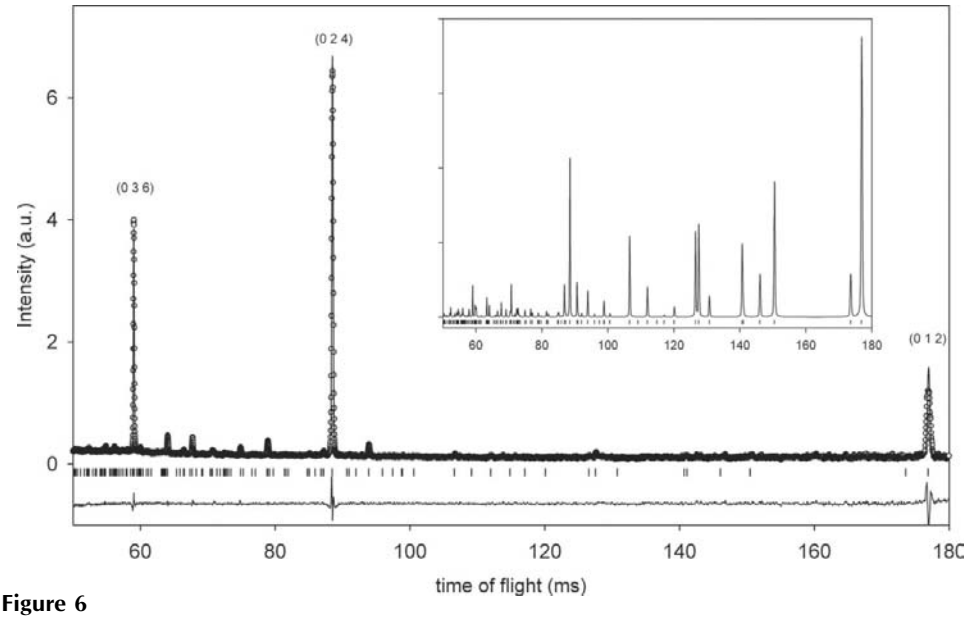


**Figure 6**
The final Pawley refinement plot of phase II at 4.8 kbar 273 K, showing observed (o), calculated (line) and difference (lower) profiles. Vertical bar markers indicate calculated Bragg peak positions. The equivalent *d*-spacing range corresponds to 1.45–5.20 Å. The calculated powder pattern based on the single-crystal X-ray structure (Shallard-Brown *et al.*, 2005) and using unit-cell and peak-width parameters from the Pawley refinement is shown in the inset.

*et al.* (1993) at 73 K, although interpreted as corresponding to an orthorhombic structure, were obtained from a metastable phase II. These data most likely correspond to the monoclinic phase III since it is often difficult to determine crystal symmetry unambiguously using spectroscopic data. The triple point for protonated cyclohexanone is clearly very close to ambient pressure, however, there are strong indications that the location of the triple point changes upon deuteration. Phase II in the current study using a deuterated compound was only rarely observed at ambient pressure. The measurements at high pressure also indicate phase II occurring in the phase III stability field observed for the $p$–$T$ diagram (see Fig. 1) derived for the protonated compound. These observations are consistent with the triple point moving to both a higher pressure and temperature owing to isotope effects. This behaviour is similar to the large isotope effect observed in the $p$–$T$ phase diagram of cyclohexene oxide, an isomer of cyclohexanone. The phase diagram for cyclohexene oxide, determined from DTA measurements (Yamamuro, 1994), is very similar to that for cyclohexanone with the triple point located at 0.114 kbar and 194 K for the protonated compound and 0.489 kbar and 200 K for the fully deuterated material. A more intriguing result from the DTA measurements is the indication that the high-pressure phase of cyclohexene oxide may in fact be an orientationally disordered plastic phase in contrast to the orientationally ordered phase II of cyclohexanone. Further study of these isomers should be revealing in terms of understanding both the critical effect of the globular nature of molecules and their complex intermolecular forces that govern the attainment of an orientationally disordered state.

## 4. Conclusions

The low-temperature phase III structure of cyclohexanone has been shown to be monoclinic in the space group $P2_1/n$. The phase II structure is orthorhombic in the space group $P2_12_12_1$ and has an increased packing density, thus may be promoted by the application of pressure. This work and the recent single-crystal X-ray study confirms previous suggestions that phase II has a restricted stability field under ambient pressure conditions.

This work has been supported by CCLRC with the provision of neutron beam time. The author also thanks Mr John Dreyer and Mr Trevor Cooper for technical assistance with the high-pressure studies.

## References

Allen, F. H., Baalham, C. A., Lommerse, J. P. M. & Raithby, P. R. (1998). *Acta Cryst.* B**54**, 320–329.
Bocelli, G. (1981). *Acta Cryst.* B**37**, 1249–1252.
Boese, R., Downs, A. J., Greene, T. M., Hall, A. W., Morrison, C. A. & Parsons, S. (2003). *Organometallics*, **22**, 2450–2457.
Boese, R. & Nussbaumer, M. (1994). *Correlations, Transformations and Interactions in Organic Chemistry*, IUCr Crystallographic Symposia, Vol. 7, edited by D. W. Jones & A. Katrusiak. Oxford University Press.
Boultif, A. & Louër, D. (1991). *J. Appl. Cryst.* **24**, 987–993.
Cremer, D. & Pople, J. A. (1975). *J. Am. Chem. Soc.* **97**, 1354–1358.
Coelho, A. A. (2000). *J. Appl. Cryst.* **33**, 899–908.
Crowe, R. W. & Smyth, C. P. (1951). *J. Am. Chem. Soc.* **73**, 5406–5411.
Devlin, F. J. & Stephens, P. J. (1999). *J. Phys. Chem. A*, **103**, 527–538.
Dillen, J. & Geize, H. J. (1980). *J. Mol. Struct.* **69**, 137–144.
Farrugia, L. J. (1997). *J. Appl. Cryst.* **30**, 565–566.
Fried, F. (1973). *Mol. Cryst. Liq. Cryst.* **20**, 1–12.
Hassel, O. & Sommerfeldt, A. M. (1938). *Z. Phys. Chem. B*, **40**, 391–395.
Huang, Y., Gilson, D. F. R. & Butler, I. S. (1993). *J. Phys. Chem.* **97**, 1998–2001.
Ibberson, R. M. (1996). *J. Appl. Cryst.* **29**, 498–500.
Ibberson, R. M., David, W. I. F. & Knight, K. S. (1992). Laboratory Report, RAL-92–031. Rutherford Appleton Laboratory, Didcot, Oxon.
Langley, C. H., Lii, J.-H. & Allinger, N. L. (2001). *J. Comput. Chem.* **22**, 1451–1475.
Nakamura, N., Suga, H. & Seki, S. (1980). *Bull. Chem. Soc. Jpn*, **53**, 2755–2761.
Pardoe, J. A. J., Norman, N. C., Timms, P. L., Parsons, S., Mackie, I., Pulham, C. R. & Rankin, D. W. H. (2003). *Angew. Chem. Int. Ed.* **42**, 571–573.
Pawley, G. S. (1981). *J. Appl. Cryst.* **14**, 357–361.

Popvitz-Biro, R., Tang, C. P., Chang, H. C., Lahav, M. & Leiserowitz, L. (1985). *J. Am. Chem. Soc.* **107**, 4043–4058.
Sayetat, F., Fertey, P. & Kessler, M. (1998). *J. Appl. Cryst.* **31**, 121–127.
Shallard-Brown, H. A., Watkin, D. J. & Cowley, A. R. (2005). *Acta Cryst.* E**61**, o2424–o2425.
Spek, A. L. (2003). *J. Appl. Cryst.* **36**, 7–13.
Spek, A. L., Duisenberg, A. J. M., van den Heuvel, H. L. A., Boer Rookhuizen, R. & Bosch, R. (1990). *Acta Cryst.* C**46**, 630–631.
Würflinger, A. (1980). *Faraday Soc. Discuss.* **69**, 146–156.
Würflinger, A. & Kreutzenbeck, J. (1978). *J. Phys. Chem. Solids*, **39**, 193–196.
Yamamuro, O. (1994). Personal communication.